Catalysis Science & Technology

Accepted Manuscript

ROYAL SOCIETY OF CHEMISTRY

www.rsc.org/catalysis

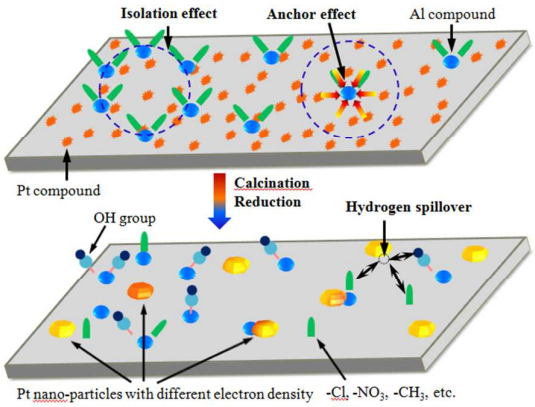

Isolation, anchor and electron-withdrawing effect of aluminum promoters improve the tetralin hydrogenation activity and sulfur-tolerance of Pt/MCM-41 catalyst greatly.

Cite this: DOI: 10.1039/c0xx00000x

www.rsc.org/xxxxxx

ARTICLE TYPE

Enhancing tetralin hydrogenation activity and sulphur-tolerance of Pt/MCM-41 catalyst with $Al(NO_3)_3$, $AlCl_3$ and $Al(CH_3)_3$

Mingjian Luo,[a,b] Qingfa Wang,*[a] Guozhu Li,[a] Xiangwen Zhang,[a] Li Wang,[a] Tao Jiang[c]

Received (in XXX, XXX) Xth XXXXXXXXX 20XX, Accepted Xth XXXXXXXXX 20XX

DOI: 10.1039/b000000x

a. Key Laboratory for Green Chemical Technology of Ministry of Education, School of Chemical Engineering and Technology, Tianjin University, Tianjin 300072, P.R. China. E-mail: qfwang@tju.edu.cn, Tel. /fax: +86 22 27892340

b. Provincial Key Laboratory of Oil & Gas Chemical Technology, College of Chemistry & Chemical Engineering, Northeast Petroleum University, Daqing 163318, P.R. China. E-mail: luomingjian@tju.edu.cn

c. College of Material Science and Chemical Engineering,Tianjin University of Science & Technology, Tianjin 300457,China.

High efficiency and sulfur-tolerant Pt-Al/MCM-41 catalysts were prepared with $Al(NO_3)_3$, $AlCl_3$ and $Al(CH_3)_3$ as promoters. The highest tetralin conversion and the best sulfur-tolerance were achieved on $Al(CH_3)_3$-promoted catalyst. The pseudo first-order rate constants of this catalyst for tetralin hydrogenation are about 2~5 and 8~10 times as high as that of the Al-free one under sulfur-free and sulfur-containing conditions, respectively. $AlCl_3$ also improves the catalytic activity and sulfur-tolerance considerablely while $Al(NO_3)_3$ has certain promotion effect on sulfur-tolerance. These promotion effects can be ascribed to (i) the anchor and isolation effects improve the platinum dispersion which benefits tetralin hydrogenation and sulfur-tolerance. (ii) The electron-withdrawing effect is $Al(NO_3)_3$ > $AlCl_3$ > $Al(CH_3)_3$, which result in a similar electron deficient $Pt^{\delta+}$ order of the catalyst. The sulfur-tolerance is in favour of electron deficient $Pt^{\delta+}$ though the tetralin hydrogenation is reversely. (iii) The acid sites and hydroxyls, especially the hydroxyls, provide additional active sites and spillover hydrogen which also contribute to the tetralin hydrogenation and sulfur-tolerance of the catalysts.

1. Introduction

Aromatic content in diesel fuel reduces the cetane number of diesel. It also increases the formation of particulates as well as the emission of NOx and polycyclic aromatic hydrocarbons (PAH). [1] Noble metal catalysts, which are high aromatic hydrogenation activity at mild reaction conditions, are important for the clean fuel production.[2-4] However, these catalysts are very sensitive to the sulfur-containing compounds presented in the feedstock. It has been proved that the supports with suitable acidity, such as SiO_2-Al_2O_3,[5-8] USY,[9] H-ZSM-5,[10, 11] mordenites,[12] H-beta,[13, 14] etc.,[15, 16] have positive effects on the hydrodearomatization activity and sulfur-tolerance of noble-metals catalysts. These effects have been attributed to the synergistic effects between acid sites and noble metal particles. Firstly, a partial of electron transfers from the metal particles to the acid sites. This electron transfer can lead to the formation of electron-deficient metal ($M^{\delta+}$), which turns lower of the strength of S-M bond and prevents the formation of metal sulfides.[5, 9, 10] Thus the noble-metal particles (active sites) are more stable. Secondly, the acid sites of the support provide additional active sites on which aromatic and sulfur-compound are hydrogenated by the spillover hydrogen.[3, 17, 18]

The acid sites of aluminosilicate are mainly provided by the Al^{3+} on the pore wall or in the framework. The post-synthesis alumination provides a convenient and flexible method to tailor the acidity of aluminosilicate.[19] Furthermore, all Al^{3+} sites of post-synthesized aluminosilicate are accessible to the supported metal and reactant. Therefore, the post-synthesis alumination offers distinct advantages over direct-synthesis with respect to investigate acid-metal or aluminum-metal interaction of supported catalysts. Park et al[20] have compared the naphthalene hydregenation activity and sulfur-tolerance of Pt catalysts supported on MCM-41, direct-synthesized Al-MCM-41 and post-synthesized Al-MCM-41. They found that Pt catalysts supported on Al-MCM-41, especially post-synthesized Al-MCM-41, have better catalytic activity and sulfur-tolerance. We also investigated the $AlCl_3$ promoted MCM-41 supported Pt catalysts with different Al-Pt interaction sequences[21] and Al/Pt ratios.[22] Results indicate that the grafting of $AlCl_3$ offers the acid sites, improves the platinum dispersion and affects the electron density of Pt particles which lead to the improvement in hydrogenation activity and sulfur-tolerance.

$Al(NO_3)_3$, $AlCl_3$ and $Al(CH_3)_3$ are three typical aluminum compounds with intrinsically different property. They surely have different interaction with MCM-41 and Pt. In this study, the Pt-Al/MCM-41 catalysts promoted by $Al(NO_3)_3$, $AlCl_3$ and $Al(CH_3)_3$ were prepared. The catalytic activity and sulfur-tolerance of the catalysts were evaluated by tetralin hydrogenation with the presence of benzothiophene. The effects

of the aluminum compounds on the properties of the catalysts as well as tetralin hydrogenation activity and sulfur-tolerance were investigated.

2 Experimental

2.1 Materials

Pure-silica MCM-41(Chemist Corporation) was calcined at 600 °C for 4 h and used as support. Anhydrous ethanol (> 99.8 wt%) and hexane were treated with 3A molecular sieve and employed as solvent. Aluminum nitrate ($Al(NO_3)_3 \cdot 9H_2O$), anhydrous aluminum chloride ($AlCl_3$) and hexachloroplatinic (IV) acid hexahydrate ($H_2PtCl_6 \cdot 6H_2O$) were dissolved in ethanol. Trimethylaluminum ($Al(CH_3)_3$) was dissolved in hexane. High purity nitrogen was used as received.

2.2 Preparation of Catalysts

Catalysts were prepared with the similar procedure described previously.[21, 22] Since $Al(CH_3)_3$ can react with ethanol, the solvent is substituted with hexane for this promoter. Catalysts were prepared as following: MCM-41 (5 g) was shifted to a three-neck flask equipped with mechanical stirrer. Anhydrous ethanol (50mL) was added to disperse the MCM-41. H_2PtCl_6-ethanol solution containing 0.05 g Pt (0.01g Pt/g MCM-41) was added to the slurry under stirring. The slurry was maintained at 75 °C for 1 h, and then ethanol was vaporized under a 200 mL/min of nitrogen stream. After the support of platinum, another 50 mL of anhydrous ethanol (or hexane) and 0.5 mmol Al-containing solvent (Al/Pt = 2, mole ratio) was added and maintained at 75 °C for 1 h, then vaporized the solvent under nitrogen stream again. The obtained powder was pressed and sieved into 16~20 mesh grain. Finally, the sample was dried at 110 °C for 2 h and calcinated at 400 °C for 4 h.

2.3 Characterization of catalysts

Prior to nitrogen adsorption-desorption isotherms, powder X-ray diffraction (XRD) and transmission electron microscope (TEM) the samples were reduced with hydrogen at atmospheric pressure and 400 °C for 4 h.

2.3.1 Nitrogen adsorption-desorption isotherms. Nitrogen adsorption-desorption isotherms were measured at -196 °C on a Micromeritics TriStar 3000 analyzer. Total surface area was calculated by multi-point Brumauer-Emmett-Teller (BET) method. The average pore size and total pore volume were calculated by Barrett-Joyner-Halenda (BJH) model.

2.3.2 Powder X-ray diffraction (XRD). Powder XRD patterns were obtained on a Rigaku D/Max 2500 instrument using Cu Kα radiation (λ = 0.1541 nm) operated at 40 kV and 200 mA. Spectra were recorded in the 2θ range 30 °~90 °.

2.3.3 Transmission electron microscope (TEM). TEM images were recorded using a JEM-2100F transmission electron microscope operating at 200 kV. Catalyst samples were dispersed and sonicated in ethanol. A drop of catalyst suspension was placed on a 230 mesh copper grid coated with carbon, and left to dry before analysis.

2.3.4 Ammonia temperature program desorption (NH_3-TPD). NH_3-TPD of the catalysts was performed on a Quantachrome ChemBET TPR/TPD chemisorptions flow analyzer. Oxidized catalyst (100 mg) was first in-situ reduced with H_2/Ar at 400 °C for 1 h (10% H_2), then cooled to 80 °C in He atmosphere. NH_3-TPD was performed from 80 °C to 600 °C at a ramp rate 15 °C/min.

2.3.5 FTIR spectra of adsorbed CO (CO-FTIR) and adsorbed pyridine (Py-FTIR). CO-FTIR and Py-FTIR spectra were recorded on a Bruker Vertex 70 FTIR spectrometer with a resolution of 4 cm^{-1}. The samples (10 mg) were pressed into self-supporting wafers (diameter 13mm), placed into an IR cell with CaF_2 windows, in-situ reduced with H_2-N_2 mixture at 400 °C for 0.5 h (50mL/min, 5% of H_2, ramp rate 2 °C/min), and then evacuated at 400 °C for 1 h. The sample was cooled to 30 °C and 100 °C before being exposed to CO and pyridine vapor, respectively. The IR spectra of adsorbed CO were recorded after exposed to 2500 Pa CO for 30 min and evacuated at 0.01 Pa for 20 min. The IR spectra of the adsorbed pyridine were recorded after being degassed at 150 °C and 280 °C for 0.5 h.

2.4 Catalyst evaluation

Catalytic activity and sulfur-tolerant evaluation were performed on a continuous down-flow fixed bed reactor. The reaction temperature was controlled by four thermocouples on the reactor wall and monitored with a thermocouple directly placed in the catalyst bed. Catalyst (1.2g, 20~16 mesh) was loaded in the isothermal zone of the fixed bed reactor. Before activity test, catalyst was in-situ reduced with 120 mL/min H_2 at 400 °C for 4 h (ramp rate: 2 °C/min). Tetralin hydrogenation was conducted at 280 °C and 5 MPa. Tetralin (20 wt.%)-*n*-dodecane solution was supplied by a Series II piston pump at 0.3 or 0.6 mL/min (0.26 or 0.52 g/min, WHSV = 13 or 26 h^{-1}). Hydrogen flow rate (120 mL/min, or 240 mL/min) was controlled by a mass flow rate controller. Tetralin (20 wt.%)-*n*-dodecane solution with 300 ppm of benzothiophene (72 ppm of sulfur) was used for the sulfur-tolerance evaluation. Blank experiment indicated that MCM-41and aluminum modified MCM-41 had none catalytic activity.

The products were quantitative analyzed on an Agilent 7890A GC equipped with an HP-PONA capillary column (50m×0.2mm×0.5μm) and an FID detector. The products were preliminarily identified by an Agilent 6890 GC-MS equipped with an HP-5MS capillary column (30m×0.25mm×0.25μm). The tetralin hydrogenation products were mainly *t*-decalin and *c*-decalin.

3 Results

3.1 Textural properties of the catalysts

Table 1. Textural properties of the reduced catalysts

catalyst	S, m^2/g	D_p, nm	V_p, cm_3/g	$d_{Pt,\ XRD}$, nm	$d_{Pt,\ TEM}$, nm
Al-free	813	3.95	0.96	6.4/5.3	4.0
$Al(NO_3)_3$-promoted	872	3.90	1.04	8.6/6.0	3.5
$AlCl_3$-promoted	804	3.92	0.94	4.8/4.6	3.1
$Al(CH_3)_3$-promoted	859	3.94	1.04	4.6/3.6	2.5

S: surface area; D_p: pore diameter; V_p: pore volume; $d_{Pt,\ XRD}$: (111)/(200) face platinum particle diameter from the XRD line broadening using the Scherrer formula; $d_{Pt,\ TEM}$: average diameter of platinum particle from TEM photograph.

The textural properties of the catalysts were characterized by

nitrogen adsorption/desorption isotherms, XRD and TEM. The results are summarized in Table 1.

Fig. 1 shows the XRD patterns of the catalysts in 2θ = 30.0°~90.0° range. The peaks at 39.7°, 46.4°, 67.7° and 81.5° are attributed to the diffraction of (111), (200), (220) and (311) faces, respectively, of crystalline face-centered cubic platinum (0). The peak broadening, which indicates that platinum is well dispersed, was observed on all catalyst especially for the $AlCl_3$ and $Al(CH_3)_3$ promoted ones. The average sizes of nano-platinum particles are estimated from (111) and (200) peaks using Scherrer formula and listed in Table 1. The sizes of nano platinum particles are also characterized by TEM (Fig. 2). The Pt particles of Al-free, $Al(NO_3)_3$-, $AlCl_3$- and $Al(CH_3)_3$-promoted catalysts are distributed mainly in 2~10, 2~5, 2~5 and 1~4 nm, respectively. The average values are 4.0, 3.5, 3.1 and 2.5 nm. According to XRD and TEM results, the platinum dispersion is improved by the aluminum promoters. The $Al(CH_3)_3$ promoted catalyst shows the highest platinum dispersion and the most uniform Pt particle size distribution. The platinum dispersions of the catalyst increases in sequence Al-free < $Al(NO_3)_3$-promoted < $AlCl_3$-promoted < $Al(CH_3)_3$-promoted.

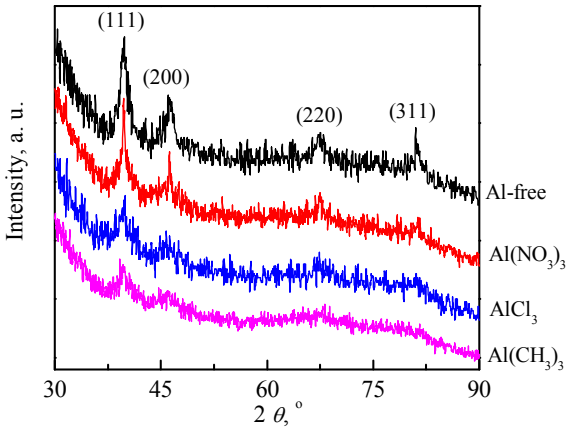

Fig. 1 XRD patterns of the catalysts

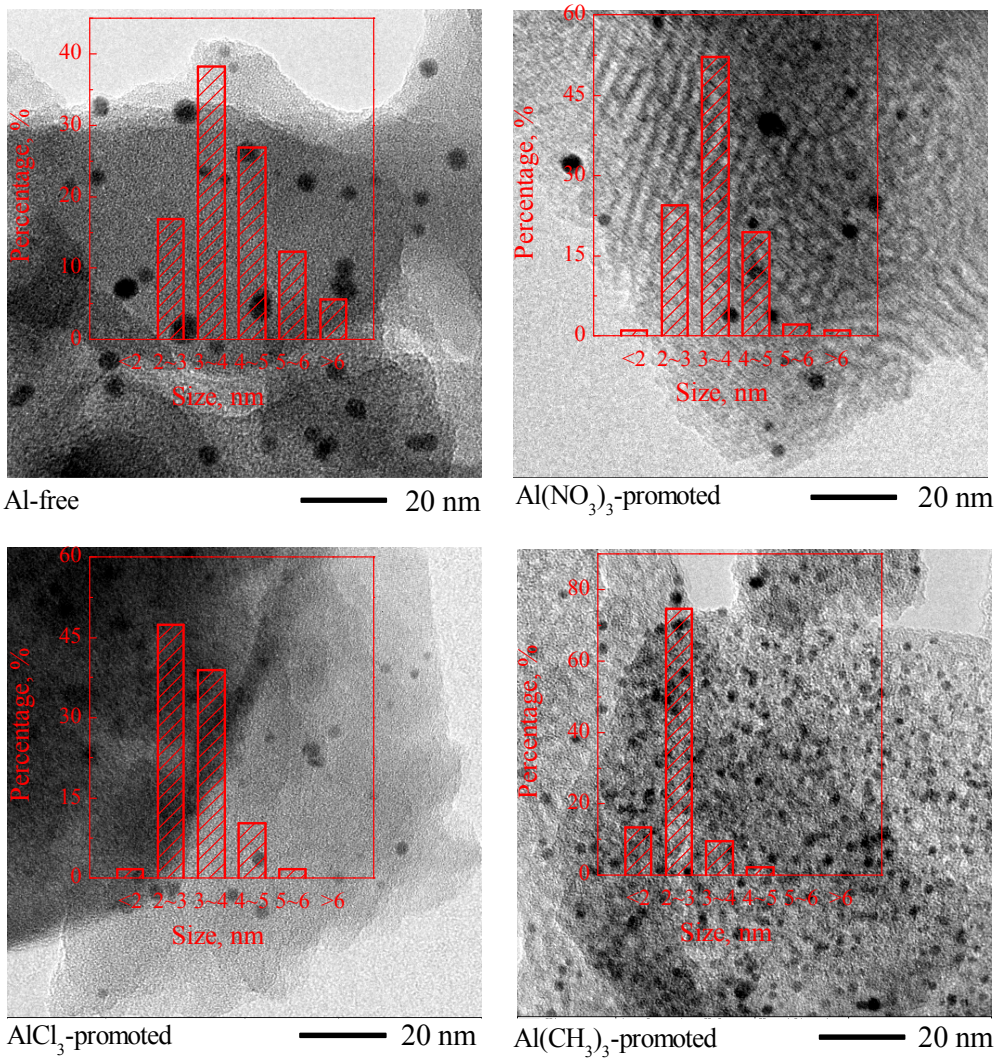

Fig. 2 TEM micrograph and platinum particle size distribution of the catalysts

3.2 Acidity of the catalyst

The acidities of the catalysts are investigated by NH_3-TPD and Py-FTIR. Fig. 3 shows the NH_3-TPD profiles of the catalysts. The MCM-41 support shows a NH_3 desorption peak below 300 °C, which should be ascribed to hydrogen-bonded NH_3 on silanol.[23, 24] The TPD profile of Al-free catalysts is similar to that of MCM-41 at low temperatue, but a little high above 300 °C. This indicates the acidity caused by platinum and residue chlorine. The aluminum promoted catalysts, which are more acidity than the Al-free one, show the similar NH_3-TPD profiles.

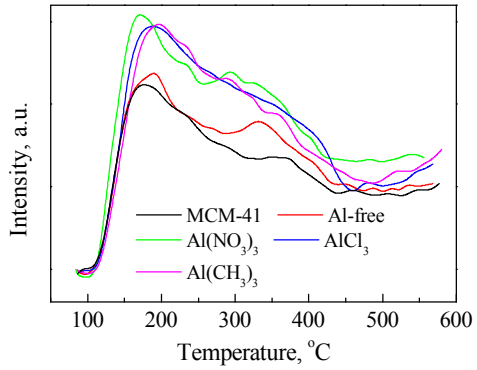

Fig. 3 The NH_3-TPD profiles of the support and catalysts

Fig. 4 shows the Py-FTIR spectra of the catalysts. The vibrations of the peaks at about 1445 and 1595 cm^{-1} are attributed to pyridine bonded to silanol or hydroxyl group; the ones at about 1453, 1575 and 1619 cm^{-1} are attributed to pyridine which is coordinately bonded on Lewis acid site; the ones at 1542 and 1637 cm^{-1} are attributed to pyridinium ion on Brönsted acid site; and the peak at 1489 cm^{-1} is contributed by three types of adsorption sites.[24-26] The amounts of Brönsted acid and Lewis acid are calculated with the molar extinction coefficients provided by Emeis.[27] Results are listed in Table 2.

The Al-free catalyst show some silanol bonded pyridine (1445 and 1595 cm^{-1}) and very little Lewis and Brönsted acid sites. Though the aluminum-contained catalysts show similar NH_3-TPD profiles, the Py-FTIR spectra are quite different, especially under low temperature. $Al(NO_3)_3$ increases the quantity and strength of these acid to some extent. $AlCl_3$, which is a Lewis acid itself, increases the quantity and strength of Lewis acid greatly, as indicated by the strong absorbance bands around 1453 and 1619 cm^{-1} at both 150 and 280 °C. $AlCl_3$ also enhances Brönsted acid (1542 and 1637 cm^{-1}) of the catalyst. $Al(CH_3)_3$, which can be hydrolyzed easily, increases the amount of hydroxyl greatly (1445 and 1595 cm^{-1}). It also improves both Lewis and Brönsted acid.

Table 2. Acid amount of the catalysts

Al promoter	B acid, μmol/g		L acid, μmol/g		Total, μmol/g	
	150 °C	280 °C	150 °C	280 °C	150 °C	280 °C
Al-free	16.0	9.7	36.1	6.6	52.2	16.3
$Al(NO_3)_3$	31.1	21.0	39.3	8.0	70.4	29.0
$AlCl_3$	51.2	25.5	60.8	23.2	112.1	48.7
$Al(CH_3)_3$	25.4	19.3	61.2	10.7	86.6	30.0

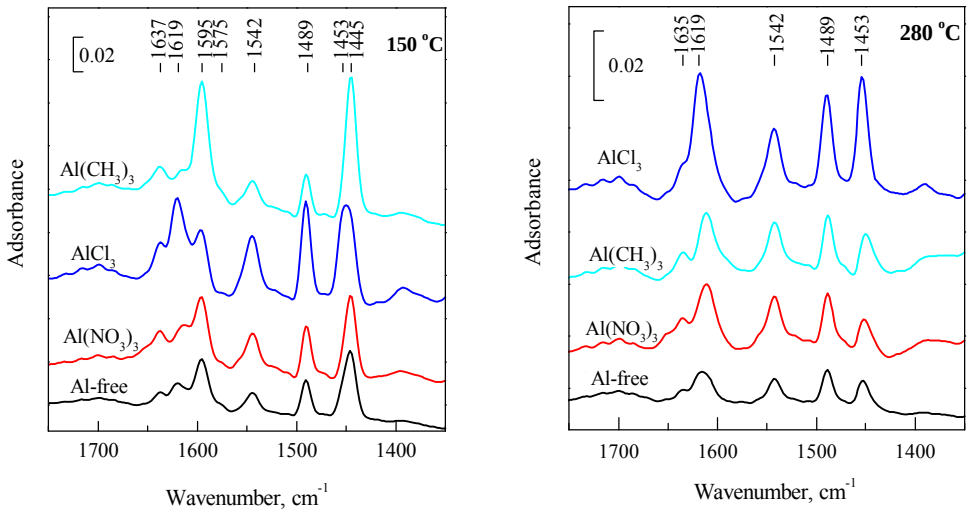

Fig. 4 Py-FTIR spectra of the catalysts

3.3 FTIR spectra of adsorbed CO

The FTIR spectra of adsorbed CO were collected to investigate the properties of active sites (Fig. 5). The strong absorbance around 2080 cm^{-1} is attributed to the CO linear bonding to platinum (Pt^0-CO) and the weak band around 1850 cm^{-1} is due to the CO bridged adsorbing on platinum (Pt^0-CO-Pt^0).[18, 28-31] Informations of band related to linear bonded CO are summarized in Table 3.

When CO is saturated (Fig. 5A), the areas of linear bonded CO band are 2.212, 2.613, 4.181 and 4.544 for the Al-free, $Al(NO_3)_3$-, $AlCl_3$- and $Al(CH_3)_3$-promoted caatalysts, respectively. These values confirmed that aluminum improve the Pt dispersion because the peak area is roughly related to the adsorbed CO amount as well as the accessible platinum amount, [32, 33] which is

roughly consistent with XRD and TEM results. However, the peak area of the $Al(CH_3)_3$-promoted catalyst was only a little higher than that of the $AlCl_3$-promoted one, though TEM image indicate that the previous catalyst has much smaller Pt nano particles than the latter one. This difference is attributed to the formation of ultra-small platinum particles in $Al(CH_3)_3$-promoted catalyst. The ultra-small Pt particle increases the percentage of defect Pt atom (corner, edge and kink sites), which lowers the CO coverage.[31] Moreover, the increase of defect platinum atom also brings in the low vibration frequency of linear-bonded CO band (Table 3). [34, 35]

Fig. 5B shows the FTIR spectra after CO evacuation. A weak shoulder peak at about 2123 cm^{-1} was observered on $AlCl_3$- and $Al(CH_3)_3$-promoted catalyst while a isolated peak at about 2165 cm^{-1} was observered on $Al(NO_3)_3$-promoted catalyst. These peaks are attributed to the CO bond to electron-deficient $Pt^{\delta+}$ particles ($Pt^{\delta+}$-CO). [36]

Table 3. Peak position and integrated area of linear bonded CO

Al promoter	Saturated		After evacuation	
	Position	Integrated area	Position	Integrated area
Al-free	2090.69	2.212	2079.31	0.331
$Al(NO_3)_3$	2088.20	2.613	2076.30	0.226
$AlCl_3$	2086.58	4.181	2076.60	0.651
$Al(CH_3)_3$	2084.89	4.544	2075.44	0.389

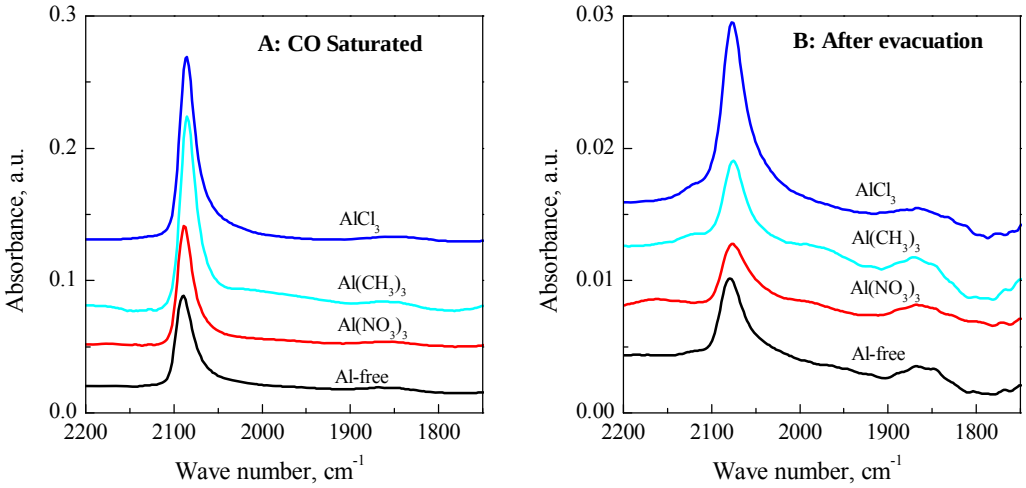

Fig. 5 CO FTIR spectra of the catalysts.

3. 4 Catalytic Performance and sulfur-tolerant mechanism discussion

The catalytic performances of the catalysts were evaluated by tetralin hydrogenation under sulfur-free and sulfur-containing conditions. Tetralin conversions as a function of time on stream are shown in Fig. 6 and the pseudo-first-order rate constants (k = - WHSV ln(1-x)) at the stable state (3 h, 7 h, 11.75 h and 15.25 h, k_1-k_4) are listed in Table 4. The relative rate constants, which are based on the reaction rate constants of Pt/MCM-41, are also calculated. With the sulfur-free feedstock at WHSV = 13 h^{-1}, the tetralin conversion of Al-free, $Al(NO_3)_3$-, $AlCl_3$- and $Al(CH_3)_3$-promoted catalysts are 95.9%, 95.1%, 99.1% and 99.7%, respectively. Tetralin conversion decreased for sulfur-containing feedstock and further decreased when WHSV is increased to 26 h^{-1}. $Al(CH_3)_3$-promoted catalyst preserved the highest tetralin conversions (92.5% and 54.5%, respectively, for the WHSV 13 and 26 h^{-1}) while the Al-free catalyst preserved the lowest ones (21.5% and 8.9%). High tetralin conversion was restored when benzothiophene was removed from the feedstock, which implies the deactivation of these catalysts is temporary. The pseudo-first-order rate constants of the $Al(CH_3)_3$-promoted catalyst are about 2~5 and 8~10 times as high as the Al-free one in tetralin hydrogenation under sulfur-free and sulfur-containing conditions, which indicate that the hydrogenation activity and sulfur-tolerance of this catalyst are greatly improved. The $AlCl_3$-promoted catalyst also show considerable improvement. Although $Al(NO_3)_3$-promoted catalyst has the lowest catalytic activity under sulfur-free conditions, it also shows positive effect on the sulfur-tolerance in a certain extent. As indicated by the k_2 and k_3 of $Al(NO_3)_3$-promoted catalyst are a little higher than that of the Al-free one.

Table 4 Pseudo-first-order rate constants of the catalyst at stable state

Al promoter	reaction rate constants, $\times10^{-3}$ s^{-1}				relative rate constant			
	k_1	k_2	k_3	k_4	k_1'	k_2'	k_3'	k_4'
Al-free	11.23	0.87	0.68	8.61	1.00	1.00	1.00	1.00
$Al(NO_3)_3$	10.97	1.00	0.76	7.03	0.98	1.14	1.13	0.82
$AlCl_3$	17.13	3.07	2.23	16.57	1.52	3.52	3.30	1.92
$Al(CH_3)_3$	22.78	9.35	5.75	41.45	2.03	10.71	8.51	4.81

Note: k = –WHSV ln(1–x); reaction conditions: 280 °C, 5 MPa, 1.2 g catalyst, k_1: 120 mL/min H_2, 0.3 mL/min liquid (13 h^{-1}), sulfur-free; k_2: 120 mL/min H_2, 0.3 mL/min liquid (13 h^{-1}), 300 ppm benzothiophene (72 ppm sulfur); k_3: 240 mL/min H_2, 0.6 mL/min liquid (26 h^{-1}), 300 ppm benzothiophene; k_4: 240 mL/min H_2, 0.6 mL/min liquid (26 h^{-1}), sulfur-free.

Table 5 The residual benzothiophene concentration at 11.5 h

Al promoter	Al-free	$Al(NO_3)_3$	$AlCl_3$	$Al(CH_3)_3$
Benzothiophene concentration, ppm	27.2	13.2	8.7	4.5

When sulfur-containing feedstock was feeding, residual benzothiophene was detected in the product at WHSV = 26 h^{-1} (Table 5). The Al-free catalyst has the highest residual benzothiophene concentration (27.2 ppm). The $Al(NO_3)_3$-

promoted catalyst, though lower catalytic activity than Al-free one, reduces the residual benzothiophene concentration to 13.2 ppm. The $Al(CH_3)_3$-promoted catalyst shows the lowest residual benzothiophene concentration (4.5 ppm).

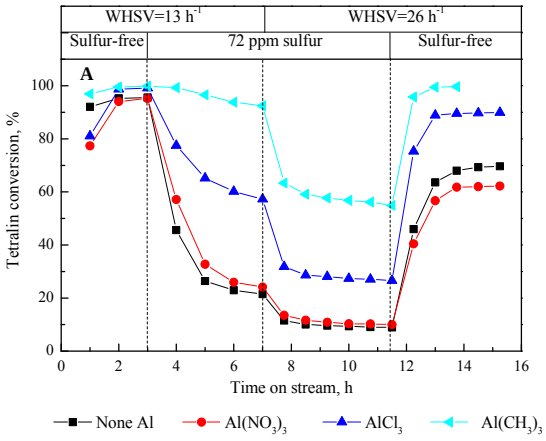

Fig. 6 Tetralin conversion with the presence and absence of 300 ppm benzothiophene (72 ppm sulfur). Reaction conditions: 280 °C, 5 MPa, 1.2 g catalyst, 120 or 240 mL/min H_2, 0.3 or 0.6 mL/min liquid ($13h^{-1}$ or $26h^{-1}$)

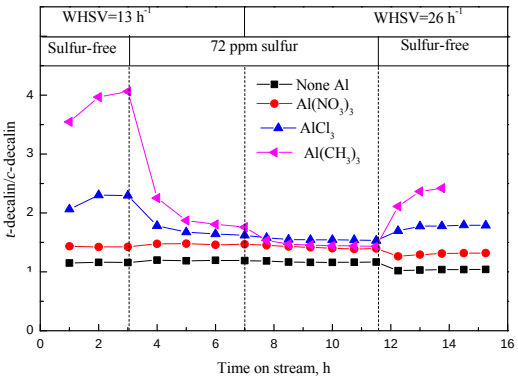

Fig. 7 Ratio of t-decalin and c-decalin in product (reaction conditions: see Fig. 6)

The four catalysts are also different in isomerization activity. Fig. 7 shows the variation of *t*-decalin/*c*-decalin in different reaction conditions. Generally, the *t*-decalin/*c*-decalin increases in order Al-free < $Al(NO_3)_3$- < $AlCl_3$- < $Al(CH_3)_3$-promoted catalyst. The *t*-decalin/*c*-decalin of Al-free and $Al(NO_3)_3$-promoted catalysts hardly change when reaction condition change. The $AlCl_3$- and $Al(CH_3)_3$-promoted catalysts have higher *t*-decalin/*c*-decalin at sulfur-free and low WHSV conditions.

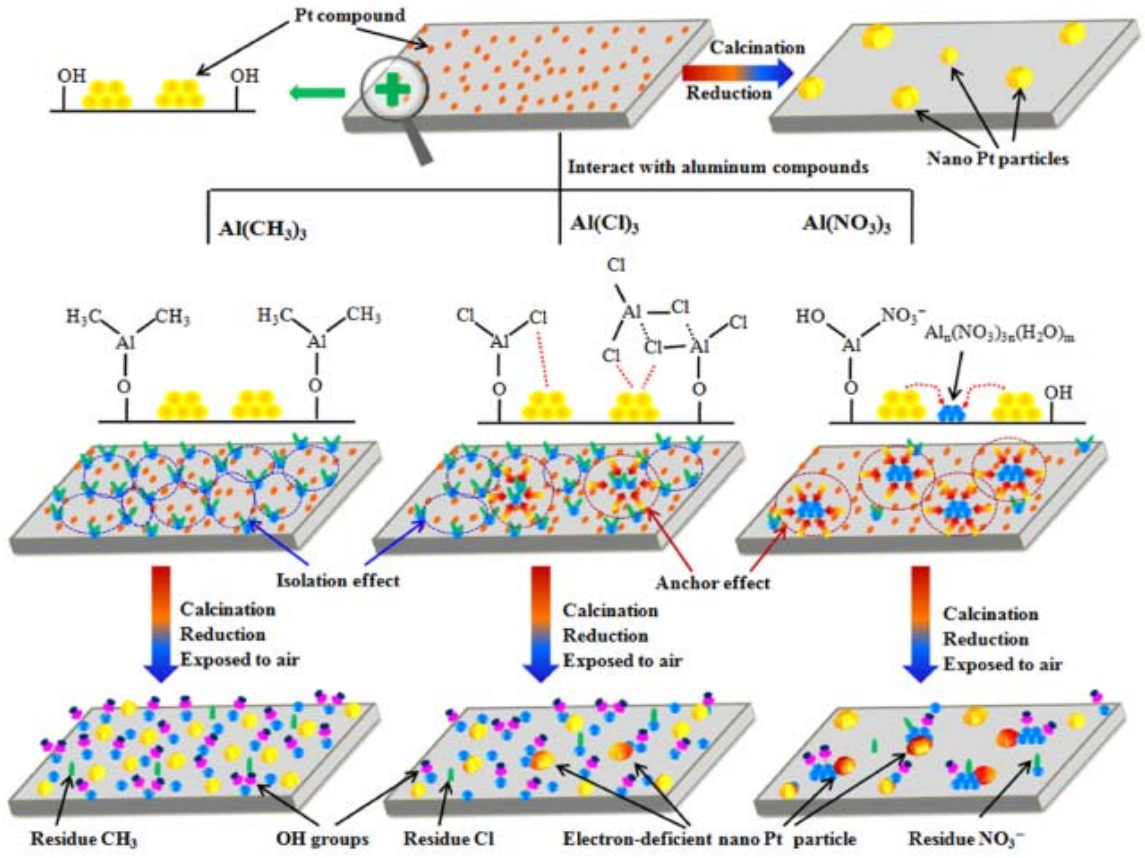

Fig. 8 Interaction mechanism of Al-promoter with the support and Pt.

4 Discussion

Due to their different properties, $Al(NO_3)_3$, $AlCl_3$ and $Al(CH_3)_3$ interact differently with the MCM-41 and the supported platinum. Accordingly, the catalysts are different in catalytic performance. We proposed an Al-Pt-support interaction mechanism as shown in Fig. 8.

4.1 Properties of the catalysts

4.1.1 Al-free catalyst. The MCM-41 surface is homogeneous for the Al-free catalyst. The interaction between the supported platinum compound and the support surface is very weak. Some platinum sinter and agglomeration to large particle during calcination and reduction. As a result, the platinum particles distributed in a broad range as well as some large prticles are observed, as indicated by the TEM image (Fig. 2). Besides, the Al-free catalyst had hardly any acid site.

4.1.2 $Al(CH_3)_3$-promoted catalyst. $Al(CH_3)_3$ is very active. It can react with the surface hydroxyl group and graft onto the support.[37-39] The morphology resistance of methyl group would isolate the platinum compound and prevent the sinter and agglomeration, which benefit the dispersing of platinum. As a result, the platinum dispersion is improved greatly and most of the platinum particles are in 2~3 nm range. The Al-CH_3 bond can be hydrolyzed easily and provide aluminum hydroxyl groups. The aluminum hydroxyl can transform into Brönsted and Lewis acid site. The formation of hydroxyl group and acid sites is verified by the Py-FTIR spectra (Fig. 4) as well as confirmed by post-synthesis alumination. [19, 37-39] In additional, the methyl group can migrate to the silicious surface.[39] The electron donor effect of methyl group increases the electron density of platinum particles, as indicated by the CO-FTIR spectra (Fig. 5).

4.1.3 $AlCl_3$-promoted catalyst. The properties of $AlCl_3$ is somewhat similar to that of $Al(CH_3)_3$. It can also react with the surface hydroxyl group and graft onto the support. However, the morphology resistance of Cl is smaller than methyl group. In additional to the isolation effect, the Cl atom also coordinated with the platinum atom which anchors the platinum compound to aluminum atom. The isolation and anchor effects improve the platinum dispersion. However, the promotion effect of $AlCl_3$ is not so efficient as $Al(CH_3)_3$. Thus the nano platinum particles are larger in $AlCl_3$-promoted catalyst than in $Al(CH_3)_3$-promoted catalyst. The hydrolization of Al-Cl bond is a little more difficult than that of Al-CH_3 bond. It is supposed that Cl was not fully removed and some Al-Cl bond remained in the catalyst.[40] As a result, the $AlCl_3$-promoted catalyst shows a large amount of Lewis acid sites (Fig. 4). The electronegative Cl and the cation Al^{3+} withdrawing the electron of platinum particle and lead to the formation of electron deficient $Pt^{\delta+}$.[28, 29]

4.1.4 $Al(NO_3)_3$-promoted catalyst. The properties of ionic compound $Al(NO_3)_3$ is essential different from the properties of $AlCl_3$ and $Al(CH_3)_3$. Though the aluminum hydrate ions can interact with the hydroxyl groups, $Al(NO_3)_3$ is mainly deposited on the support surface. This argument is verified by the NH_3-TPD and Py-FTIR results. The $Al(NO_3)_3$-promoted catalyst shows similar amount of acid sites as $AlCl_3$ and $Al(CH_3)_3$-promoted ones with the small probe molecule NH_3 (Fig. 3), but much less amount of acid sites than the latter ones with large probe molecule pyridine (Fig. 4). For the same reason, the $Al(NO_3)_3$ have hardly any isolation effect. However, $Al(NO_3)_3$ is similar properties with H_2PtCl_6, thus the platinum compound can be anchored around the aluminum. As a result, the platinum dispersion is improved in certain extent by $Al(NO_3)_3$. Moreover, the electron-withdrawing effect of Al^{3+} pulls the electron from the adjacent platinum particles and leads to the formation of most electron deficient $Pt^{\delta+}$.

In summary, the aluminum promoters affect on the acid property, the platinum dispersion and electron property of platinum particles. For the acid property, $Al(CH_3)_3$ increases the amount of hydroxyl group greatly; $AlCl_3$-promoted catalyst has the greatest amount of Lewis acid sites; and $Al(NO_3)_3$ enhances the acidity of catalyst in certain extent. The aluminum promoters improve the platinum dispersion via isolation and anchor effects. The $Al(CH_3)_3$ shows the best isolation effect and improves the platinum dispersion greatly; the $AlCl_3$ has both isolation and anchor effects, it also increases the platinum dispersion considerable; the $Al(NO_3)_3$ anchors the platinum compound around it and improves the platinum dispersion a little. The interaction between aluminum and platinum leads to the formation of electron deficient $Pt^{\delta+}$. The electron density of nano platinum particles in the catalysts should increased in sequence $Al(NO_3)_3$-promoted < $AlCl_3$-promoted < Al-free ≈ $Al(CH_3)_3$-promoted. This comment is verified by the CO-FTIR results. Similarly, V G Baldovino-Medrano[41] stated that Pd particles from chlorided precursor are more electron deficient than from organometallic precursor.

4.2 Correlation between properties and performances

4.2.1 Catalytical activity

The improvement in platinum dispersion, which implies more active sites, is sure to affect on the catalytic activity.[42] Combining the XRD, TEM and CO-FTIR results with the tetralin conversions and pseudo-first order rate constants of the catalysts, it is obviously that the higher the platinum dispersion, the better tetralin hydrogenation activity. Thus it is easy to understand and conclude that the tetralin hydrogenation activity is first related to the platinum dispersion.

The second factor that affect the catalytic activity is the electron density of Pt particles. The Al-free catalyst, though lower platinum dispersion than $Al(NO_3)_3$-promoted one, have higher tetralin hydrogenation activity than the latter catalyst. The pseudo-first-order rate constants of $Al(CH_3)_3$-promoted catalyst is twice as high as that of $AlCl_3$-promoted one while the integrated area of linear bonded CO is only 9% higher. As discussed above, the electron density of platinum in $Al(CH_3)_3$-promoted catalyst is higher than that in $AlCl_3$-promoted one and the Pt particles of $Al(NO_3)_3$-promoted catalyst is the most electron deficient. [21, 43, 44] Accordingly, the tetralin hydrogenation is in favour of less electron deficient platinum particles.

Thirdly, the acid sites and hydroxyls provide additionally active sites and favour spillover hydrogen which also contribute to hydrogenation activity.[45, 46] Additionally, it is reasonable to suppose that the promotion of hydroxyls is better than the effect of Lewis and Brönsted acid sites since the $Al(CH_3)_3$-promoted catalyst possesses the largest amount of hydroxyls and the best catalytic activity.

4.2.2 Sulfur-tolerance

Due to its benzenic ring, thiophenic rings and electronegative

sulfur atom, benzothiophene is more competitive adsorbable to the active site than tetralin.[47-49] The competitive adsorption of benzothiophene, which hinders the adsorption and hydrogenation of tetralin, is the main reason that dedicated to the deactivation of the catalyst.[21, 22] As showed in Table 5, the Al-free catalyst has the lowest benzothione hydrogenation activity, and then $Al(NO_3)_3$-, $AlCl_3$-promoted catalyst. The $Al(CH_3)_3$-promoted catalyst has the best benzothiophene hydrogenation activity. Combining with the tetralin conversion and pseudo-first-order rate constants under sulfur-containing condition, it can be concluded that the better the benzothiophene hydrogenation activity, the better the sulfur tolerance.

It is obviously that the improvement in platinum dispersion is one of the reasons for the enhancement of sulfur-tolerance of the catalyst. The lowest residual benzothiophene concentration of $Al(CH_3)_3$-promoted catalyst is mainly attributed to its high platinum dispersion. However, contrary to the tetralin hydrogenation, the benzothiophene hydrogenation activity and the sulfur-tolerance of the catalyst is rather related to the electron deficient platinum particles ($Pt^{\delta+}$) and acidity than to the platinum dispersion.[5, 6, 10, 22, 41, 47] Due to its electronnegative, benzothiophene is in favour of electron deficient $Pt^{\delta+}$. Simultaneously, the $Pt^{\delta+}$ pulls the electrons of benzenic ring and thiophenic ring, and thereby destabilizes the rings which promotes the hydrogenation of thiophenic ring and the scission of S–C bond. Therefore, benzothiophene hydrogenation is promoted by the electron-deficient $Pt^{\delta+}$. As a result, the electron deficient $Al(NO_3)_3$ -promoted catalyst, though lower tetralin hydrogenation activity under sulfur-free condition than Al-free one, has a much lower residual benzothiophene concentration as well as higher tetralin conversion under sulfur-containing condition than the latter catalyst. Thus the sulfur-tolerance is in favor with electron deficient $Pt^{\delta+}$, which is opposite to the tetralin hydrogenation. The acid sites and hydroxyl provide additionally active sites and spillover hydrogen which also contribute to the sulfur-tolerance of the catalysts.[3, 7, 8, 17, 45, 46]

4.2.3 Isomerization active sites

The catalysts are also different in isomerization activity. Fig. 7 showed the ratio of *t*-decalin to *c*-decalin vs. time on stream. All Al-containing catalysts have higher *t*-decalin to *c*-decalin ratio than Al-free one. The *t*-decalin to *c*-decalin ratio hardly changed for the Al-free and $Al(NO_3)_3$-promoted catalysts while $AlCl_3$- and $Al(CH_3)_3$-promoted ones have more *t*-decalin in the product at sulfur-free condition. Additionally, three Al-containing catalysts are similar *t*-decalin to *c*-decalin ratios under sulfur-containing conditions. It is established that the isomerization activity is related to two types of activity sites: the conventional acid sites and the platinum sites. The isomerization activity of acid site is insensitive to the sulfur and tetralin conversion. However, since aromatic and thiophenic rings are more competitively adsorbable to the metal sites, isomerization activity of the platinum sites is suppressed by the present tetralin and benzothiophene. When tetralin is completely converted to decalin ($AlCl_3$- and $Al(CH_3)_3$-promoted catalyst under sulfur-free conditions), the isomerization of *t*-decalin to *c*-decalin become dynamically favored.[20, 50]

5. Conclusions

The $Al(NO_3)_3$, $AlCl_3$ and $Al(CH_3)_3$ promoters improve the platinum dispersions, affect on the electron state of platinum particles and provide additional acid sites and hydroxyls. The anchor and isolation effects of $AlCl_3$ and $Al(CH_3)_3$, especially $Al(CH_3)_3$, improve the platinum dispersion of the catalyst greatly, which benefits tetralin hydrogenation and sulfur-tolerance. The electron-withdrawing effect is $Al(NO_3)_3 > AlCl_3 > Al(CH_3)_3$. Thus Pt particles in $Al(NO_3)_3$-promoted catalyst is the most electron deficient, and then $AlCl_3$-promoted. The $Al(CH_3)_3$-promoted one is the least electron deficient since its electron donor methyl group. The sulfur-tolerance is in favour of electron deficient $Pt^{\delta+}$ though the tetralin hydrogenation is reversely. The grafting of aluminum and hydrolyzation of $AlCl_3$ and $Al(CH_3)_3$ increase acid sites and hydroxyls. These sites provide additional active sites and spillover hydrogen which also contribute to the tetralin hydrogenation and sulfur-tolerance. All three aluminum promoters improve the sulfur-tolerance while $AlCl_3$ and $Al(CH_3)_3$ benefits both tetralin hydrogenation activity and sulfur-tolerance, and $Al(CH_3)_3$ is the best.

Acknowledgements

The financial supports by National Natural Science Fund of China (Grant No. 90916022) are gratefully acknowledged. The authors also acknowledge the support of Analysis Center of Tianjin University.

References

1. Worldwide Fuel Charter, E. A. M. Association, A. o. A. Manufacturers, E. M. Association and J. A. M. Association, 4th, September 2006.
2. R. G. Leliveld and S. E. Eijsbouts, *Catal. Today*, 2008, 130, 183-189.
3. C. Song and X. L. Ma, *Appl. Catal. B: Environ.*, 2003, 41, 207-238.
4. B. H. Cooper and B. B. L. Donnis, *Appl. Catal. A: Gen.*, 1996, 137, 203-223.
5. A. M. Venezia, V. L. Parola, B. Pawelec and J. L. G. Fierro, *Appl. Catal. A: Gen.*, 2004, 264, 43-51.
6. A. E. Coumans, D. G. Poduval, J. A. R. van Veen and E. J. M. Hensen, *Appl. Catal. A: Gen.*, 2012, 411, 51-59.
7. S. Nassreddine, L. Massin, M. Aouine, C. Geantet and L. Piccolo, *J. Catal.*, 2011, 278, 253-265.
8. S. Nassreddine, S. Casu, J. L. Zotin, C. Geantet and L. Piccolo, *Catalysis Science & Technology*, 2011, 1, 408-412.
9. H. Yasuda, T. Sato and Y. Yoshimura, *Catal. Today*, 1999, 50, 63-71.
10. K. B. Sidhpuria, P. A. Parikh, P. Bahadur, B. Tyagi and R. V. Jasra, *Catal. Today*, 2009, 141, 12-18.
11. M. Göhlich, S. Böttcher, K. Räuchle and W. Reschetilowski, *Catal. Commun.*, 2011, 12, 757–760.
12. L. J. Simon, J. G. van Ommen, A. Jentys and J. A. Lercher, *Catal. Today*, 2002, 73, 105-112.
13. T. Tang, C. Yin, L. Wang, Y. Ji and F.-S. Xiao, *J. Catal.*, 2008, 257, 125-133.
14. T. Tang, C. Yin, L. Wang, Y. Ji and F.-S. Xiao, *J. Catal.*, 2007, 249, 111-115.
15. S. Albertazzi, N. Donzel, M. Jacquin, D. J. Jones, M. Morisi, J. Roziére and A. Vaccari, *Catal. Lett.*, 2004, 96, 157-164.
16. P. Castaño, A. Gutiérrez, B. Pawelec, J. L. G. Fierro, A. T. Aguayo and J. M. Arandes, *Appl. Catal. A: Gen.*, 2007, 333, 161-172.
17. S. D. Lin and M. A. Vannice, *J. Catal.*, 1993, 143, 563-572.
18. B. Pawelec, R. Mariscal, R. M. Navarro, S. van Bokhorst, S. Rojas and J. L. G. Fierro, *Appl. Catal. A: Gen.*, 2002, 225, 223-237.
19. R. Mokaya, in *Series on Chemical Engineering*, ed. T. K. Wei, Imperial College Press, London, 2004, vol. 4, ch. Chapter 14 Surface alumination of mesoporous silicates, pp. 427-463.
20. K. C. Park, D. J. Yim and S. K. Ihm, *Catal. Today*, 2002, 74, 281-290.

21. M. Luo, Q. Wang, G. Li, X. Zhang, L. Wang and L. Han, , *Catalysis Communication*, 2013, 35, 6-10.
22. M. Luo, Q. Wang, G. Li, X. Zhang and L. Wang, *Catal. Lett.*, 2013, 145, 454-462.
23. F. Lónyi and J. Valyon, *Microporous Mesoporous Mater.*, 2001, 47, 293-301.
24. M. C. Kung and H. H. Kung, *Catalysis Reviews*, 1985, 27, 425-460.
25. A. Corma, *Chem. Rev.*, 1995, 95, 559-614.
26. E. P. Parry, *J. Catal.*, 1963, 2, 371-379.
27. C. A. Emeis, *J Catal*, 1993, 141, 347-354.
28. R. M. Navarro, B. Pawelec, J. M. Trejo, R. Mariscal and J. L. G. Fierro, *J. Catal.*, 2000, 189, 184-194.
29. S. Albertazzi, G. Busca, E. Finocchio, R. Glöckler and A. Vaccari, *J. Catal.*, 2004, 223, 372-381.
30. K. I. Hadjiivanov and G. N. Vayssilov, *Advances in Catalysis*, 2002, 47, 307-511.
31. P. Hollins, *Surf. Sci. Rep.*, 1992, 16, 51-94.
32. M. A. Albiter and F. Zaera, *Langmuir*, 2010, 26, 16204–16210.
33. R. A. Shigeishi and D. A. King, *Surf. Sci.*, 1976, 58, 379-396.
34. A. Davydov, *Molecular Spectroscopy of Oxide Catalyst Surfaces*, Wiley, 2003.
35. A. A. Solomennikov, Y. A. Lokhov, A. A. Davydov and Y. A. Ryndin, *Kinet. Catal.*, 1979, 589-594.
36. , !!! INVALID CITATION !!!
37. Y. Oumi, H. Takagi, S. Sumiya, R. Mizuno, T. Uozumi and T. Sano, *Micropor Mesopor Mat*, 2001, 44, 267-274.
38. S. Sumiya, Y. Oumi, T. Uozumi and T. Sano, *J Mater Chem*, 2001, 11, 1111-1115.
39. J. H. Li, J. A. DiVerdi and G. E. Maciel, *J Am Chem Soc*, 2006, 128, 17093-17101.
40. K. Ito, M. A. Ohshima, H. Kurokawa, K. Sugiyama and H. Miura, *Catal. Commun.*, 2002, 3, 527-531.
41. V. G. Baldovino-Medrano, E. M. G. P. Eloyb and S. A. G. a. A. Centeno, *Catalysis Today*, 2010, 150, 186-195.
42. A. M. Venezia, R. Murania, V. La Parola, B. Pawelec and J. L. G. Fierro, *Appl. Catal. A: Gen.*, 2010, 383, 211-216.
43. T. Visser, T. A. Nijhuis, A. M. J. van der Eerden, K. Jenken, Y. Y. Ji, W. Bras, S. Nikitenko, Y. Ikeda, M. Lepage and B. M. Weckhuysen, *J. Phys. Chem. B*, 2005, 109, 3822-3831.
44. A. M. J. van der Eerden, T. Visser, A. Nijhuis, Y. Ikeda, M. Lepage, D. C. Koningsberger and B. M. Weckhuysen, *JACS*, 2005, 127, 3272-3273.
45. H. Yang, H. L. Chen, J. W. Chen, O. Omotoso and Z. Ring, *J. Catal.*, 2006, 243, 36-42.
46. F. Roessnera and U. Roland, *J. Mol. Catal. A: Chem.*, 1996, 112, 401-412.
47. V. G. Baldovino-Medrano, P. Eloy, E. M. Gaigneaux, S. A. Giraldo and A. Centeno, *J. Catal.*, 2009, 267, 129-139
48. H. Yang, C. Fairbridge and Z. Ring, *Energy & Fuels*, 2003, 17, 387-398.
49. F. Besenbacher, M. Brorson, B. S. Clausen, S. Helveg, B. Hinnemann, J. Kibsgaard, J. Lauritsen, P. G. Moses, J. K. Nørskov and H. Topsøe, *Catal. Today*, 2008, 130, 86-96.
50. A. D. Schmitz, G. Bowers and C. Song, *Catal. Today*, 1996, 31, 45-56.